Biophysical Reports

REPORT

Temperature-dependent elastic properties of DNA

Marc Rico-Pasto[1] and Felix Ritort[1,2,*]

[1]Small Biosystems Lab, Condensed Matter Physics Department, University of Barcelona, Barcelona, Spain and [2]Institut de Nanociència i Nanotecnologia (IN2UB), Universitat de Barcelona, Barcelona, Spain

ABSTRACT Knowledge of the elastic properties, e.g., the persistence length or interphosphate distance, of single-stranded (ss) and double-stranded (ds) DNA under different experimental conditions is critical to characterizing molecular reactions studied with single-molecule techniques. While previous experiments have addressed the dependence of the elastic parameters upon varying ionic strength and contour length, temperature-dependent effects are less studied. Here, we examine the temperature-dependent elasticity of ssDNA and dsDNA in the range 5°C–50°C using a temperature-jump optical trap. We find a temperature softening for dsDNA and a temperature stiffening for ssDNA. Our results highlight the need for a general theory explaining the phenomenology observed.

SIGNIFICANCE The accurate knowledge of the persistence and contour lengths of single-stranded and double-stranded DNA is critical to characterize the thermodynamics of molecular reactions studied through single-molecule techniques. Here, using a novel temperature-jump optical trap, we find a temperature softening for dsDNA and a temperature stiffening for ssDNA.

INTRODUCTION

DNA is the biomolecule in charge of storing the genetic information of living organisms. *In vivo*, DNA is commonly found in its double-stranded (dsDNA) conformation forming the double helix (1). However, dsDNA dissociates into two single-strands (ssDNA) in many biological processes, such as DNA replication, reparation, or transcription (2,3). Since the invention of single-molecule techniques, e.g., optical tweezers (4,5), the elastic properties of dsDNA and ssDNA molecules have been investigated (6,7). In force spectroscopy experiments, where mechanical forces are used to unfold and fold DNA/RNA molecules and proteins, a detailed characterization of the elastic properties of biomolecules is crucial to obtain valuable information, such as bending energies (8,9), folding free energy (10–12), and binding energies (12–14). The elasticity of semi-flexible biopolymers, such as DNA, is commonly modeled with the worm-like chain (WLC) ideal elastic model and its interpolation formula (15,16). This model describes the elastic response using two parameters: L_p and d_b. L_p is the persistence length over which correlations in the direction of the tangent of the polymer decay, and d_b is the inter-phosphate distance, i.e., the distance between consecutive phosphates in the nucleotide chain. Originally introduced by Krakty and Porod in 1949 as a discretized version of the elastic rod model (17), the WLC is mathematically equivalent to the Heisenberg model in a one-dimensional chain in a magnetic field solved by McGurn and Scalapino back in 1975 (18). It is only after the seminal experiments by Bustamante and coworkers in 1992 that a full force-extension curve for dsDNA became available by visualizing the motion of fluorescent DNA molecules attached to micron-sized beads acted on by magnetic and hydrodynamic forces (19). While the experimental data were fitted to a freely jointed chain model, satisfactory results were only obtained 2 years later by using the WLC model (20).

Previous studies investigated the elastic parameters of DNA by varying the length of the molecules and the ionic condition at room temperature (298 K). The values of the inter-phosphate distance at room temperature reported from single-molecule experiments match with those of X-ray crystallography, $d_b = 6$ Å for ssDNA and $d_b = 3$ Å for dsDNA, for different polymer lengths (21,22) and ionic strengths (23,24). Moreover, the persistence length exhibits different behavior when varying the length of the polymer. On

Submitted May 17, 2022, and accepted for publication July 20, 2022.

*Correspondence: ritort@ub.edu

Editor: Jorg Enderlein.

https://doi.org/10.1016/j.bpr.2022.100067

the one hand, at standard conditions (298 K and 1 M NaCl concentration), the persistence length for long ssDNA chains (> 100 bases) are roughly equal to d_b, ($L_p = 0.7$ nm), whereas for short chains (< 100 bases), $L_p = 1.3$ nm (16,25–27). For sufficiently long dsDNA chains (> 50 bp), $L_p = 50$ nm, while for molecules shorter than the persistence length (< 50 bp), finite length effects are important. The effective or apparent persistence length decreases with length being in the range ∼2–20 nm (15,21,22).

Here, we investigate the temperature dependence of the elastic properties of ssDNA and dsDNA using a temperature-jump optical trap (Fig. 1) (28–30). We measure the temperature- and force-dependent molecular extension from unzipping and stretching experiments to determine the elastic properties using the inextensible WLC model. To study the ssDNA, we have investigated sequence dependence effects on three DNA hairpins formed by 24, 32, and 44 bases of different guanine-cytosine (GC) content (100% GC content in poly(GC), ∼14% GC content in poly(AT), and 50% GC content in a mixed content hairpin). On the other hand, we pull on a 24 kbp dsDNA in a wide temperature range of 5°C–50°C to characterize dsDNA elasticity.

MATERIALS AND METHODS

DNA synthesis

The DNA hairpins (poly(GC), poly(AT), and mixed) have been synthesized using a protocol described in reference (25). To minimize stacking interactions along the ssDNA, the sequence of the stem consists of purine-pyrimidine dinucleotide steps. Briefly, the molecular construction used in our experiments has two identical dsDNA handles acting as spacers to prevent non-specific interactions between the beads and the molecule under investigation. To do so, a primary oligonucleotide containing the sequence of the hairpin flanked by one strand of the DNA handles is hybridized with a second oligonucleotide to form the dsDNA handles. For the dsDNA segment, we cut a segment of 24,805 bp from a commercially available λ phage.

Single-molecule experiments

We tether the molecular construction between two beads, one coated with streptavidin, and the other coated with anti-digoxigenin. The beads specifically bind to biotin- and digoxigenin-labeled ends of the molecular construct. The streptavidin bead is immobilized at the tip of a glass micro-pipette by air suction, while the anti-digoxigenin bead is captured in the optical trap (see Fig. 1 *a* and *d*). The relative distance between the center of the optical trap and the micro-pipette, denoted as λ, is the control parameter of the experiments. In unzipping and stretching experiments, the optical trap moves back and forth relative to the micro-pipette. All the experiments carried out in this study are done in a buffer solution of 7.5 pH with 1 M NaCl, 10 mM EDTA and 10 mM Tris.

Temperature-jump optical trap

Details of the temperature-jump optical trap can be found in reference (28). Briefly, a collimated heating laser (1435 nm wavelength) is used to uniformly heat the area surrounding the optical trap. By water absorption, the temperature is locally raised from 25°C (room temperature) to 50°C. The miniaturized instrument is placed inside an icebox kept at 5°C and heated from this basal temperature up to 25°C. In this way, the available temperature ranges from 5°C to 50°C.

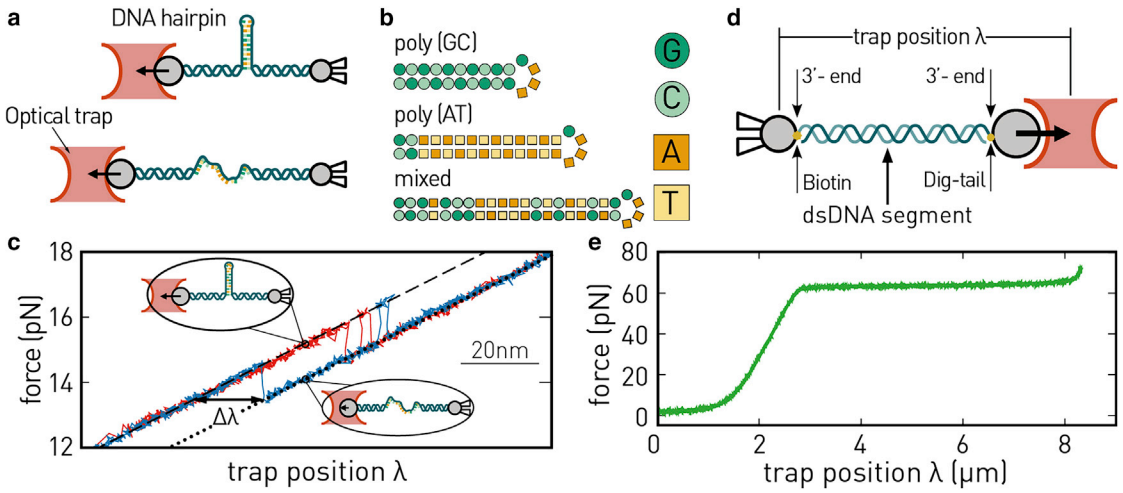

FIGURE 1 Schematic of the experiments. (*a*) Experimental setup for pulling DNA hairpins. (*b*) Sequences of the three investigated DNA hairpins: poly(GC), poly(AT), and mixed. Poly(GC) is formed by 10 GC bp in the stem, poly(AT) has two GC bp and 12 AT bp, and the mixed one has ∼50% GC bp. The three hairpins end in a *GAAA* tetraloop. (*c*) Force-distance curve (FDC) measured at 25°C in a buffer solution at 7.5 pH with 1 M NaCl, 10 mM EDTA, and 10 mM Tris for the mixed hairpin showing the two force branches. Black dashed line corresponds to the elastic response of the system when the hairpin is folded. Black dotted line is the elastic response of the system when the molecule is unfolded. It has been calculated using the elastic properties of ssDNA reported in the literature (16,27). The difference in trap position at a given force ($\Delta\lambda$) is used to determine the force-dependent molecular extension. (*d*) Experimental setup for the dsDNA experiments. (*e*) FDC for a 24 kbp DNA molecule measured at 298 K in a buffer solution at 7.5 pH with 1 M NaCl, 10 mM EDTA, and 10 mM Tris. The overstretching transition is observed as a force plateau at ∼67 pN (15).

RESULTS AND DISCUSSION

ssDNA

We have carried out unzipping experiments to determine the force- and temperature-dependent molecular extension of ssDNA, x_{ssDNA}, and derived its elastic properties. In unzipping experiments, the optical trap is repeatedly moved away from and toward the micropipette to mechanically unfold/fold the hairpins (Fig. 2 *a*). At low forces, the three hairpins are in their native state (N), while at high forces, hairpins are unfolded (U) in their ssDNA conformation. The unfolding $(N \rightarrow U)$ and folding $(U \rightarrow N)$ events are observed as force rips in the force-distance curves (FDCs; see Fig. 1 *c*). *N*- and *U*-force branches are defined as the FDCs when the molecule is in N and U, respectively. Therefore, by measuring the difference in trap position at fixed force values $\Delta\lambda(f)$, we derive the difference in molecular extension between the ssDNA $(x_{ssDNA}(f))$ and the folded conformations of the hairpins $(x_d(f))$, which has its extension given by the helix diameter,

$$\Delta\lambda(f) = x_{ssDNA}(f) - x_d(f). \quad (1)$$

To extract x_{ssDNA} from Eq. 1, we model $x_d(f)$ using the freely jointed chain. The extension $x_d(f)$ is analogous to the projected orientation of a rigid dipole under a magnetic field. The extension of the rigid dipole equals the thickness of the B-DNA (helix diameter), i.e., 2 nm length. We assume that the helix diameter is constant with T. Fig. 2 *b* shows the measured $x_{ssDNA}(f)$ at 25°C for the three DNA hairpins: poly(GC) (green), poly(AT) (yellow), and mixed (red). The solid lines are the expected behavior using parameters reported in the literature (16,26,27). As expected from the FDCs (Fig. 2 *a*), each hairpin shows the elastic response of the ssDNA over different force regimes (Fig. 2 *b*). In addition, the normalized extension x_{ssDNA} by the total number of bases does not show visible sequence effects (Fig. 2 *c*).

To determine the temperature-dependent elastic properties of ssDNA, we have fitted the force versus x_{ssDNA} to the inextensible WLC model and its interpolation formula (20),

$$f = \frac{k_B T}{4L_p}\left(\left(1 - \frac{x}{Nd_b}\right)^{-2} + 4\frac{x}{Nd_b} - 1\right), \quad (2)$$

with f as the measured force, x ($\equiv x_{ssDNA}$) the molecular extension, N the number of bases, k_B the Boltzmann constant, and T the temperature. The temperature-dependent molecular extension of the ssDNA has been directly determined from the FDCs recorded at different temperatures (Fig. 2 *d*) using Eq. 1. We have determined the temperature dependence of L_p and d_b by fitting the force-extension curves (FECs) to Eq. 2, leaving L_p and d_b as free parameters.

Fig. 2 *e* shows the FECs (symbols) with the fits to Eq. 2 (solid lines) for the three hairpins at all temperatures

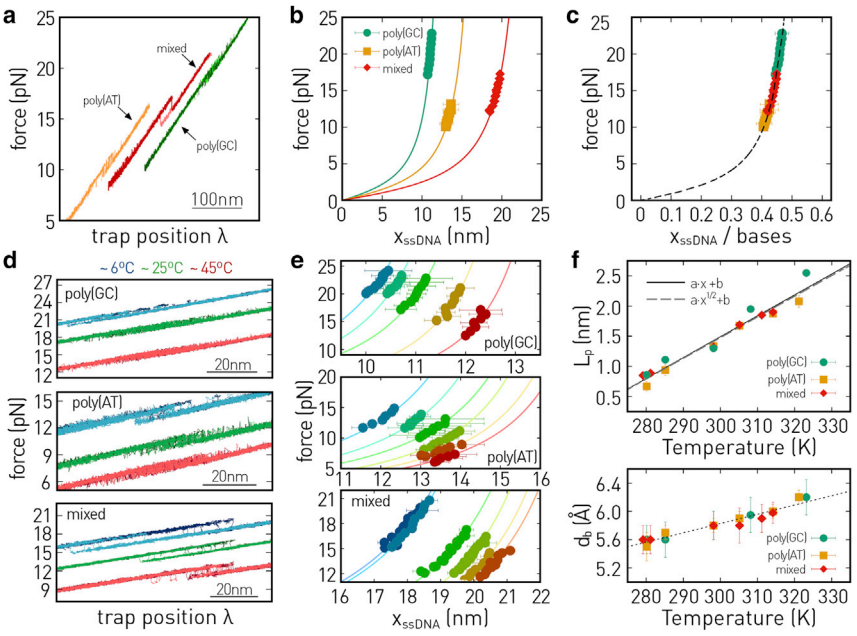

FIGURE 2 Force-extension curves of ssDNA. (*a*) Unzipping (*dark colors*) and rezipping (*light colors*) FDC for each molecule: poly(GC) (*green*), poly(AT) (*yellow*), and mixed (*red*). (*b*) Molecular extension at 25°C of poly(GC) (*green*), poly(AT) (*yellow*), and mixed (*red*) hairpins. Solid line is the expected behavior using the WLC model with the elastic properties reported in the literature (16,27). (*c*) A plot of force versus normalized (per base) ssDNA extension does not show sequence effects. (*d*) Unzipping (*dark colors*) and rezipping (*light colors*) FDCs measured at three selected $\boldsymbol{T}$: ~6°C (*blue*), ~25°C (*green*), and ~45°C (*red*). (*e*) Force versus ssDNA molecular extension at the explored temperatures: 7°C, 12°C, 25°C, 35°C, and 50°C for poly(GC), 7°C, 12°C, 25°C, 32°C, 41°C, and 48°C for poly(AT), and 6°C, 8°C, 17°C, 25°C, 32°C, 42°C, and 45°C for the mixed hairpin. (*f*) Top: temperature-dependent persistence length $(\boldsymbol{L_p})$ for the three hairpins. We do not appreciate differences between the linear fit, $\boldsymbol{L_p(T) = aT + b}$ (*black solid line*), and the Debye-Hückel dependence, $\boldsymbol{L_p(T) = aT^{1/2} + b}$ (*gray dashed line*). Bottom: measured $\boldsymbol{d_b}$ together with a linear fit (*dashed line*). The change of $\boldsymbol{L_p}$ with $\boldsymbol{T}$ is ~20 times larger than for $\boldsymbol{d_b}$, the latter being roughly constant with $\boldsymbol{T}$.

(7°C, 12°C, 25°C, 35°C, and 50°C for poly(GC), 7°C, 12°C, 25°C, 32°C, 41°C, and 48°C for poly(AT), and 6°C, 8°C, 17°C, 25°C, 32°C, 42°C, and 45°C for mixed hairpins). Note that for a fixed force value, the extension of the ssDNA becomes larger (and therefore stiffer) upon increasing temperature. L_p shows a strong temperature dependence for all sequences (Fig. 2 *f*, *top*), whereas the inter-phosphate distance is weakly T dependent (Fig. 2 *f*, *bottom*). Both parameters, d_b and L_p, have been fit to a linear dependence: $L_p(T) = aT + b$ and $d_b(T) = aT + b$. Fitting parameters are $a = 0.28 \pm 0.01$ Å/K and $b = -7.2 \pm 0.4$ nm for L_p and $a = 0.016 \pm 0.002$ Å/K and $b = 0.13 \pm 0.05$ nm for d_b. From the a values, we conclude that L_p changes with T roughly 20 times faster than d_b does. Therefore, the inter-phosphate distance can be taken as constant. If L_p is related to a Debye-Hückel length, one would expect a $T^{1/2}$ dependence (31). No significant differences are observed between a linear fit and the Debye-Hückel dependence: $L_p(T) = aT^{1/2} + b$, $a = 1.00 \pm 0.05$ nm/K$^{1/2}$, and $b = -15.9 \pm 0.7$ nm (Fig. 2 *f*-top).

dsDNA

In dsDNA pulling experiments, the force is exerted on opposite labeled 3′ ends in each complementary ssDNA strand (Fig. 1 *d*). Upon stretching and releasing, FDCs of dsDNA are quasi-reversible in the range 1–80 pN (Fig. 1 *e*). FDCs present three regimes (Fig. 1 *e*). In the first regime, $f < 5$ pN, stretching is opposed by the entropic elasticity. The second regime, $5 < f < 60$ pN, is dominated by the enthalpic contribution to dsDNA bending. In this regime, FDCs become steep, and small changes in the molecular extension are translated into large changes in the measured force. The third regime occurs at high forces, $f \sim 67$ pN at 25°C, where a force plateau is observed. The plateau corresponds to the overstretching transition of DNA (15), where the double helix unwinds into a new structure (S-DNA). S form consists of a ladder interspersed by fried ssDNA stretches due to pre-existing nicks (32,33).

In Fig. 3 *a*, we show FDCs at different temperatures, 9°C (dark blue), 15°C (light blue), 25°C (green), 38°C (brown), and 45°C (red). We notice that the overstretching force is remarkably affected by T, decreasing upon heating. Fig. 3 *b* shows the force at the mid-point of the overstretching plateau (f_{over}) as a function of T. The measured T dependence of f_{over} in the range 7°C–50°C agrees with previous experiments carried out by other groups in different temperature ranges (34–36).

The entropic regime ($f < 5$ pN) is also T dependent. Fig. 3 *b* shows FECs at different T obtained after converting the trap position (λ) into dsDNA molecular extension $(x_{\text{dsDNA}}(f))$. To derive $x_{\text{dsDNA}}(f)$, we have subtracted the bead displacement from the measured trap-pipette distance λ,

$$\lambda(f) = x_{\text{dsDNA}}(f) + \frac{f}{k_b} + \lambda_0, \tag{3}$$

where λ_0 is an arbitrary origin, and k_b is the bead's stiffness. We determine the value of k_b from the unfolding trajectories shown in the previous section using Eq. 3 but for DNA hairpins, i.e., by including the handles extension of the hairpin constructs,

$$\lambda(f) = x_{\text{ssDNA}}(f) + \frac{f}{k_b} + x_h(f) + \lambda_0. \tag{4}$$

In Eq. 4, the elastic response of the dsDNA handles $(x_h(f))$ was derived using the elastic properties reported in the literature (25), and $x_{\text{ssDNA}}(f)$ is derived as explained in the previous section. From $x_h(f)$ and

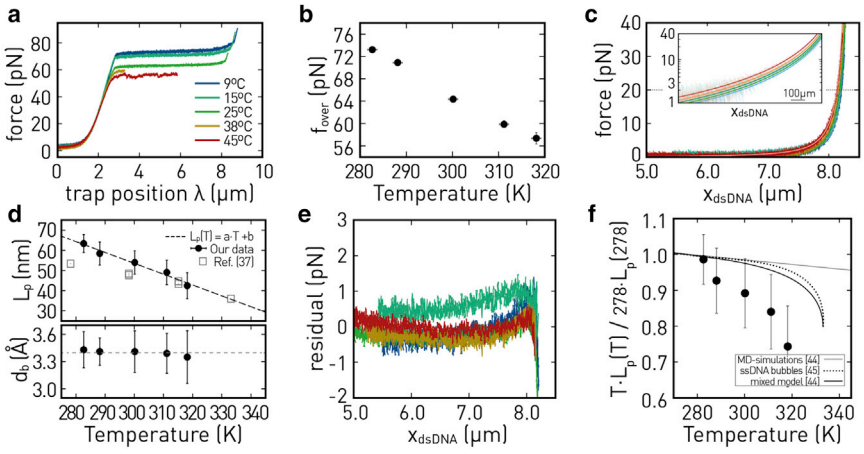

FIGURE 3 Stretching dsDNA. (*a*) FDCs obtained at different temperatures using the 24 kbp dsDNA molecule. (*b*) Average force at the overstretching plateau as a function of temperature. (*c*) Measured FECs at 9°C (*dark blue*), 15°C (*light blue*), 25°C (*green*), 38°C (*brown*), and 45°C (*red*). The lines denote the fits to the WLC model. (*d*) Temperature-dependent persistence length (*top*) and inter-phosphate distance (*bottom*). The dashed line in on the top is a linear fit (average value). The black circles are our results, and the gray squares are the results obtained in (37). (*e*) Residuals defined as the difference between the measured force and the fitted one as a function of x_{dsDNA}. (*f*) Experimental persistence length multiplied by temperature and rescaled by its value at 278 K (symbols) together with predictions reported in the literature (lines); see text for details.

$x_{\mathrm{ssDNA}}(f)$, we fitted the *U*-force branch to derive the value of k_b that best matches Eq. 4 with the experimental data.

FECs show a systematic T dependence (Fig. 3 *c*, *inset*). At a given force, the higher the T, the lower the molecular extension $x_{\mathrm{dsDNA}}(f)$. This trend indicates that L_p for dsDNA decreases with T. This behavior is the opposite of what we have observed for ssDNA (Fig. 2 *e*). To derive the T dependence of the elastic parameters, L_p and d_b, we have fitted the inextensible WLC model, Eq. 2, in the force range 0–20 pN. The derived L_p and d_b are shown in Fig. 3 *d*, and the fitting FECs are shown in Fig. 3 *c* as lines. We notice that L_p is strongly affected by the temperature (Fig. 3 *d*, *top*). Like for the ssDNA, L_p shows a linear dependence $L_p(T) = aT + b$ but with a negative slope $a = -0.54 \pm 0.05$ nm/K. Remarkably, the results shown in Fig. 3 *d* (top) agree with experiments carried out at 10 mM $MgCl_2$ in cyclization of short DNA fragments (37), proving that the empirical 1:100 rule for mono and divalent salts is satisfied. This empirical rule has been previously observed in the elasticity of ssDNA (38) and ssRNA (39) in the hybridization energies in DNA (28) and RNA in melting experiments of oligos (40,41). Recently, the salt empirical rule has been demonstrated at the level of individual nearest neighbor base pairs in mechanical unzipping experiments (42). Moreover, d_b is roughly constant with an average inter-phosphate distance $d_b \simeq 0.34$ nm, which agrees with X-ray crystallographic measurements (Fig. 3 *d*, *bottom*). Notice, however, that the inter-phosphate distance is slightly reduced when the temperature is increased. This temperature behavior agrees with recent molecular dynamics simulations (43). In Fig. 3 *e*, we show the residuals of the fits as a function of x_{dsDNA}. Notice that residuals are < 1 pN in the fitted range. The drop in the residuals observed above 8.0 μm are deviations from the inextensible WLC model.

CONCLUSIONS

We have investigated the elastic response of ssDNA and dsDNA at different temperatures (5°C–50°C) from pulling experiments. By mechanically unzipping DNA hairpins, we derive the elastic response of ssDNA from the difference in extension between the folded and unfolded branches. Experiments on hairpins of varying GC content show that the persistence length of ssDNA is sequence independent. This has been demonstrated for sequences of purine-pyrimidine dinucleotide motifs, where stacking effects should be small. For dsDNA, the elasticity has been measured by stretching a 24 kbp halve from λ-phage DNA. FECs of ssDNA and dsDNA have been fitted to the inextensible WLC model. The model describes the elasticity of semi-flexible biopolymers using two parameters: the persistence length, L_p, over which polymer orientations become decorrelated, and the inter-phosphate distance, d_b, between consecutive phosphates in the backbone.

We have found that L_p is strongly affected by T for both ssDNA and dsDNA, in agreement with previous studies. Interestingly, whereas ssDNA becomes stiffer, dsDNA becomes softer with T. It has been shown that L_p for semi-flexible polymers have two contributions,

$$L_p = L_p^0 + L_p^{\mathrm{el}}, \tag{5}$$

where L_p^0 is the intrinsic persistence length, and L_p^{el} is the electrostatic correction. In general, both L_p^0 and L_p^{el} are temperature dependent. While L_p^0 depends on the mechanical deformation properties of the polymer, i.e., its bending and torsional rigidity, L_p^{el} is a screening collective effect due to water and ions in the surrounding media. The temperature dependence of L_p^0 can be described through the WLC model relation,

$$B = k_B T L_p^0, \tag{6}$$

where B is the bending rigidity, *a priori* temperature-independent parameter. L_p^{el} is proportional to the screening Debye-Hückel length (λ_D). For a one-component salt, it is given by

$$\lambda_D = \left(\frac{\varepsilon k_B T}{c q^2}\right)^{1/2}, \tag{7}$$

with q as the ion charge, c the ion number density, and ε the dielectric constant. We hypothesize that our results for ssDNA and dsDNA can be described by Eq. 5 depending on whether L_p^{el} (ssDNA) or L_p^0 is dominant (dsDNA). In ssDNA, the temperature dependence of $L_p(T)$ is well fitted by the function $L_p(T) = L_p^0 + \alpha\sqrt{T}$, with $L_p^0 = -16$ nm. A negative L_p^0 is physically meaningless, suggesting that the $\sqrt{T}$ fit is only valid in the limited explored temperature range. An increasing L_p with T for ssDNA indicates that electrostatic interactions are determinant. In fact, previous unzipping experiments in kbp-long DNA hairpins and 8–100 residue homopolymeric ssDNAs in solution showed that L_p follows a Debye-Hückel behavior, $L_p \propto 1/c^{1/2}$ (26,38). Interestingly, a similar T dependence has been reported for polypeptide chains (30). In contrast, the decrease of $L_p(T)$ with T for dsDNA is compatible with a temperature-independent bending rigidity, B, through the WLC model relation (Eq. 6). Fig. 3 *f* shows the persistence length of dsDNA multiplied by temperature and rescaled by its value at 278 K together with

the expected behavior for a double-helical structure determined from molecular dynamics (44), a prediction model where denaturated ssDNA bubbles are present (45), and a mixed model (44).

Finally, the inter-phosphate distance d_b is practically temperature independent for ssDNA and dsDNA in the explored temperature range. For ssDNA, d_b increases linearly with T, with a slope $\sim$20 times smaller than the slope for L_p. Therefore, we can take $d_b = 0.58 \pm 0.01$ nm as constant. The same conclusion holds for dsDNA where $d_b = 0.34 \pm 0.01$ nm. Both d_b values agree with those measured from X-ray crystallographic experiments.

The evidence accumulated during the last decades on the temperature and salt dependencies of the elastic parameters in ssDNA and dsDNA molecules highlight the need to develop a general theory based on polyelectrolyte models that explains both behaviors. At present, we have a qualitative understanding based on the theory of semi-flexible polymers and electrostatic models such as the electrical double-layer theory (46), the Odijk-Skolnick-Fixman theory (47,48), or the tight-binding ion model (49), among others. It would be interesting to extend this temperature study to other salt conditions to better understand the interplay between salt and temperature. Moreover, it would be helpful to explore whether the same phenomenology also holds for RNA.

AUTHOR CONTRIBUTIONS

M.R.-P. and F.R. designed the research. M.R.-P. carried out all experiments and analyzed the data. M.R.-P. and F.R. wrote the article.

ACKNOWLEDGMENTS

The authors acknowledge financial support from the Spanish Research Council (PID2019-111148GB-I00), and the ICREA Academia prize 2018 (Catalan Government).

DECLARATION OF INTERESTS

The authors declare no competing interests.

REFERENCES

1. Watson, J. D., and F. H. Crick. 1953. Molecular structure of nucleic acids: a structure for deoxyribose nucleic acid. *Nature.* 171:737–738.
2. Alberts, B. 2003. DNA replication and recombination. *Nature.* 421:431–435.
3. Friedberg, E. C., G. C. Walker, …, R. D. Wood. 2005. DNA Repair and Mutagenesis. American Society for Microbiology Press.
4. Ashkin, A. 1970. Acceleration and trapping of particles by radiation pressure. *Phys. Rev. Lett.* 24:156–159.
5. Ashkin, A., J. M. Dziedzic, …, S. Chu. 1986. Observation of a single-beam gradient force optical trap for dielectric particles. *Opt. Lett.* 11:288–290.
6. Bustamante, C., S. B. Smith, …, D. Smith. 2000. Single-molecule studies of DNA mechanics. *Curr. Opin. Struct. Biol.* 10:279–285.
7. Camunas-Soler, J., M. Ribezzi-Crivellari, and F. Ritort. 2016. Elastic properties of nucleic acids by single-molecule force spectroscopy. *Annu. Rev. Biophys.* 45:65–84.
8. Bustamante, C., Z. Bryant, and S. B. Smith. 2003. Ten years of tension: single-molecule DNA mechanics. *Nature.* 421:423–427.
9. Le, T. T., and H. D. Kim. 2014. Probing the elastic limit of DNA bending. *Nucleic Acids Res.* 42:10786–10794.
10. Collin, D., F. Ritort, …, C. Bustamante. 2005. Verification of the Crooks fluctuation theorem and recovery of RNA folding free energies. *Nature.* 437:231–234.
11. Ritort, F. 2006. Single-molecule experiments in biological physics: methods and applications. *J. Phys. Condens. Matter.* 18:R531–R583.
12. Idili, A., F. Ricci, and A. Vallée-Bélisle. 2017. Determining the folding and binding free energy of DNA-based nanodevices and nanoswitches using urea titration curves. *Nucleic Acids Res.* 45:7571–7580.
13. Li, Y., M. Qin, …, W. Wang. 2014. Single molecule evidence for the adaptive binding of DOPA to different wet surfaces. *Langmuir.* 30:4358–4366.
14. Camunas-Soler, J., A. Alemany, and F. Ritort. 2017. Experimental measurement of binding energy, selectivity, and allostery using fluctuation theorems. *Science.* 355:412–415.
15. Smith, S. B., Y. Cui, and C. Bustamante. 1996. Overstretching B-DNA: the elastic response of individual double-stranded and single-stranded DNA molecules. *Science.* 271:795–799.
16. Viader-Godoy, X., M. Manosas, and F. Ritort. 2021. Sugar-pucker force-induced transition in single-stranded DNA. *Int. J. Mol. Sci.* 22:4745.
17. Nelson, P. 2004. Biological Physics. WH Freeman.
18. McGurn, A. R., and D. J. Scalapino. 1975. One-dimensional ferromagnetic classical-spin-field model. *Phys. Rev. B.* 11:2552–2558.
19. Smith, S. B., L. Finzi, and C. Bustamante. 1992. Direct mechanical measurements of the elasticity of single DNA molecules by using magnetic beads. *Science.* 258:1122–1126.
20. Bustamante, C., J. F. Marko, …, S. Smith. 1994. Entropic elasticity of lambda-phage DNA. *Science.* 265:1599–1600.
21. Seol, Y., J. Li, …, M. Betterton. 2007. Elasticity of short DNA molecules: theory and experiment for contour lengths of 0.6–7μm. *Biophys. J.* 93:4360–4373.
22. Chen, Y.-F., D. P. Wilson, …, J.-C. Meiners. 2009. Entropic boundary effects on the elasticity of short DNA molecules. *Phys. Rev. E Stat. Nonlin. Soft Matter Phys.* 80:020903.
23. Zhang, C., H. Fu, …, X. Zhang. 2019. The mechanical properties of RNA-DNA hybrid duplex stretched by magnetic tweezers. *Biophys. J.* 116:196–204.
24. Fu, H., C. Zhang, …, X.-H. Zhang. 2020. Opposite effects of high-valent cations on the elasticities of DNA and RNA duplexes revealed by magnetic tweezers. *Phys. Rev. Lett.* 124:058101.
25. Forns, N., S. de Lorenzo, …, F. Ritort. 2011. Improving signal/noise resolution in single-molecule experiments using molecular constructs with short handles. *Biophys. J.* 100:1765–1774.
26. Sim, A. Y. L., J. Lipfert, …, S. Doniach. 2012. Salt dependence of the radius of gyration and flexibility of single-stranded DNA in solution probed by small-angle x-ray scattering. *Phys. Rev. E Stat. Nonlin. Soft Matter Phys.* 86:021901.
27. Alemany, A., and F. Ritort. 2014. Determination of the elastic properties of short ssDNA molecules by mechanically folding and unfolding DNA hairpins. *Biopolymers.* 101:1193–1199.

28. de Lorenzo, S., M. Ribezzi-Crivellari, …, F. Ritort. 2015. A temperature-jump optical trap for single-molecule manipulation. *Biophys. J.* 108:2854–2864.
29. Rico-Pasto, M., I. Pastor, and F. Ritort. 2018. Force feedback effects on single molecule hopping and pulling experiments. *J. Chem. Phys.* 148:123327.
30. Rico-Pasto, M., A. Zaltron, …, F. Ritort. 2022. Molten globule–like transition state of protein barnase measured with calorimetric force spectroscopy. *Proc. Natl. Acad. Sci. USA.* 119. e2112382119.
31. Brydges, D. C., and P. A. Martin. 1999. Coulomb systems at low density: a review. *J. Stat. Phys.* 96:1163–1330.
32. Williams, M. C., J. R. Wenner, …, V. A. Bloomfield. 2001. Effect of pH on the overstretching transition of double-stranded DNA: evidence of force-induced DNA melting. *Biophys. J.* 80:874–881.
33. Wenner, J. R., M. C. Williams, …, V. A. Bloomfield. 2002. Salt dependence of the elasticity and overstretching transition of single DNA molecules. *Biophys. J.* 82:3160–3169.
34. Williams, M. C., J. R. Wenner, …, V. A. Bloomfield. 2001. Entropy and heat capacity of DNA melting from temperature dependence of single molecule stretching. *Biophys. J.* 80:1932–1939.
35. Zhang, X., H. Chen, …, J. Yan. 2012. Two distinct overstretched DNA structures revealed by single-molecule thermodynamics measurements. *Proc. Natl. Acad. Sci. USA.* 109:8103–8108.
36. Zhang, X., H. Chen, …, J. Yan. 2013. Revealing the competition between peeled ssDNA, melting bubbles, and S-DNA during DNA overstretching by single-molecule calorimetry. *Proc. Natl. Acad. Sci. USA.* 110:3865–3870.
37. Geggier, S., A. Kotlyar, and A. Vologodskii. 2011. Temperature dependence of DNA persistence length. *Nucleic Acids Res.* 39:1419–1426.
38. Bosco, A., J. Camunas-Soler, and F. Ritort. 2014. Elastic properties and secondary structure formation of single-stranded DNA at monovalent and divalent salt conditions. *Nucleic Acids Res.* 42:2064–2074.
39. Bizarro, C. V., A. Alemany, and F. Ritort. 2012. Non-specific binding of Na+ and Mg 2+ to RNA determined by force spectroscopy methods. *Nucleic Acids Res.* 40:6922–6935.
40. Schroeder, S. J., and D. H. Turner. 2000. Factors affecting the thermodynamic stability of small asymmetric internal loops in RNA. *Biochemistry.* 39:9257–9274.
41. Heilman-Miller, S. L., D. Thirumalai, and S. A. Woodson. 2001. Role of counterion condensation in folding of the Tetrahymena ribozyme. I. Equilibrium stabilization by cations. *J. Mol. Biol.* 306:1157–1166.
42. Rissone, P., C. V. Bizarro, and F. Ritort. 2022. Stem–loop formation drives RNA folding in mechanical unzipping experiments. *Proc. Natl. Acad. Sci. USA.* 119. e2025575119.
43. Dohnalová, H., T. Dršata, …, F. Lankaš. 2020. Compensatory mechanisms in temperature dependence of DNA double helical structure: bending and elongation. *J. Chem. Theory Comput.* 16:2857–2863.
44. Meyer, S., D. Jost, …, R. Everaers. 2013. Temperature dependence of the DNA double helix at the nanoscale: structure, elasticity, and fluctuations. *Biophys. J.* 105:1904–1914.
45. Theodorakopoulos, N., and M. Peyrard. 2012. Base pair openings and temperature dependence of DNA flexibility. *Phys. Rev. Lett.* 108:078104.
46. Hunter, R. J. 2001. Foundations of Colloid Science. Oxford University Press.
47. Odijk, T. 1977. Polyelectrolytes near the rod limit. *J. Polym. Sci. Polym. Phys. Ed.* 15:477–483.
48. Skolnick, J., and M. Fixman. 1977. Electrostatic persistence length of a wormlike polyelectrolyte. *Macromolecules.* 10:944–948.
49. Tan, Z.-J., and S.-J. Chen. 2005. Electrostatic correlations and fluctuations for ion binding to a finite length polyelectrolyte. *J. Chem. Phys.* 122:044903.